Analysis of Refractive ^{16}O + ^{16}O Elastic Scattering at E_{lab} = 480 MeV

Yong Joo Kim and Hye Young Moon

Department of Physics, Cheju National University, Cheju 690-756

We analyzed the elastic scattering of ^{16}O + ^{16}O system at E_{lab} = 480 MeV by using the Coulomb-modified eikonal approximation. The calculations lead to a reasonable agreements with the observed data of this system. The refractive oscillatory structures observed in the elastic angular distributions could be explained due to the interference between the near- and far-side amplitudes. The presence of the nuclear rainbow is evidenced through classical deflection function. The strong real and weak imaginary potentials are found to be essential to describe the refractive ^{16}O + ^{16}O elastic scattering at E_{lab} = 480 MeV.

I. INTRODUCTION

Generally, the heavy-ion elastic scattering is dominated by strong absorption. In this situation, the nuclear potential can be obtained ambiguously, because the scattering data are sensitive to the surface of interaction region. However, data from the lighter heavy-ion systems at intermediate energies is dominated by diffraction and exhibit a typical Fraunhöfer diffraction pattern in the small angle regions. Beyond this regions the cross section exhibits a structureless exponential falloff. Such a behavior was identified as being a typical refraction effect generated by the nuclear rainbow. The nuclear rainbows seen in the elastic cross section uniquely determined the major features of the optical potential for these heavy-ion systems.

In recent, there are several attempts [1–4] to explain the nuclear rainbow situation in the elastic scattering between lighter heavy-ions. The ^{16}O + ^{16}O elastic scattering have been measured at 22 MeV/u in a large angular range with high accuracy, and these data show a nuclear rainbow structure for the first time in heavy-ion scattering with unambiguous clarity [1]. Ingemarsson et al. [2] has discussed the effects of the real potential on the absorption of lighter heavy-ions using the "effective potential". The first- and third-order non-eikonal corrections to the Glauber model

have been developed to know the possibility of observing a bright interior in the nucleus "viewed" by intermediate energy alpha particles (E_α=172.5 MeV), as a probe for the ^{58}Ni nucleus [3].

For many years, the eikonal approximation has been widely used for the description of the heavy-ions elastic scattering. A number of studies [5–9] have been made to describe elastic scattering processes between heavy ions within the framework of the eikonal approximation methods. Aguiar et al. [8] has discussed different schemes devised to extended the eikonal approximation to the regime of low bombarding energies in heavy-ion collisions. In our previous paper [7, 9], we have presented the first- and second-order corrections to the zero-order eikonal phase shifts for heavy-ion elastic scatterings based on Coulomb trajectories of colliding nuclei and it has been applied satisfactorily to the ^{16}O + ^{40}Ca and ^{16}O + ^{90}Zr systems at E_{lab}=1503 MeV.

The elastic scattering data of ^{16}O + ^{16}O system at E_{lab}= 480 MeV has been measured and analyzed within the optical model using the density-dependent folding potential [10]. These data show the presence of strong refractive effects in the angular distributions. It is interesting to apply the Coulomb-modified eikonal approximation formalism to the refractive ^{16}O + ^{16}O elastic scattering. In

this paper, we reproduce the elastic scattering of $^{16}O + ^{16}O$ systems at $E_{lab}= 480$ MeV by using the phase shift analysis based on Coulomb-modified eikonal phase shift. The near-side and far-side decompositions of the cross sections due to Fuller's relationship[11] are presented. The features of optical potential needed for fitting the observed data are also discussed. In section II, we provide the Coulomb-modified eikonal approximation formalism based on Coulomb trajectories of colliding nuclei. Section III contains results and discussions. Finally, concluding remarks are presented in section IV.

II. COULOMB-MODIFIED EIKONAL APPROXIMATION

In the case of elastic scattering between two identical spinless nuclei, the general expression of the differential cross section is given by the following formula

$$\frac{d\sigma}{d\Omega} = |f(\theta) + f(\pi - \theta)|^2, \qquad (1)$$

where elastic scattering amplitude $f(\theta)$ is given by the equation

$$f(\theta) = f_R(\theta) + \frac{1}{ik}\sum_{L=0}^{\infty}(L + \frac{1}{2})\exp(2i\sigma_L)$$
$$\times (S_L^N - 1)P_l(\cos\theta). \qquad (2)$$

Here $f_R(\theta)$ is the usual Rutherford scattering amplitude, k is the wave number and $\sigma_L = \arg\Gamma(L + 1 + i\eta)$ the Coulomb phase shifts. The nuclear S-matrix elements S_L^N can be expressed by the nuclear phase shifts δ_L

$$S_L^N = \exp(2i\delta_L). \qquad (3)$$

In this work, we use the eikonal phase shift based on the Coulomb trajectories of the colliding nuclei. If there is a single turning point in the radial Schrödinger equation, the WKB expression for the nuclear elastic phase shifts δ_L^{WKB}, taking into account the deflection effect due to Coulomb field, can be written as [12, 13]

$$\delta_L^{WKB} = \int_{r_t}^{\infty} k_L(r)\,dr - \int_{r_c}^{\infty} k_c(r)\,dr, \qquad (4)$$

where r_t and r_c are the turning points corresponding to the local wave numbers $k_L(r)$ and $k_c(r)$ given by

$$k_L(r) = k\left[1 - \left(\frac{2\eta}{kr} + \frac{L(L + 1)}{k^2 r^2} + \frac{U(r)}{E}\right)\right]^{1/2}, \qquad (5)$$

and

$$k_c(r) = k\left[1 - \left(\frac{2\eta}{kr} + \frac{L(L + 1)}{k^2 r^2}\right)\right]^{1/2}, \qquad (6)$$

where η is the Sommerfeld parameter, and $U(r)$ the nuclear potential. The distance of closest approach r_c is given by

$$r_c = \frac{1}{k}[\eta + [\eta^2 + L(L + 1)]^{1/2}]. \qquad (7)$$

In the high-energy limit, we can consider the nuclear potential as a perturbation. Thus, the turning point r_t may be taken to be coincident with r_c and

$$k_L(r) - k_c(r) = k_c(r)\left[1 - \frac{2\mu U(r)}{\hbar^2 k_c^2(r)}\right]^{1/2} - k_c(r)$$
$$\simeq -\frac{\mu V_n(r)}{\hbar^2 k_c(r)}. \qquad (8)$$

If we substitute Eq.(8) into Eq.(4) and rearrange the terms, we can find that the phase shift in terms of r_c instead of L, is given by

$$\delta_L(r_c) \simeq \int_{r_c}^{\infty} [k_L(r) - k_c(r)]dr$$
$$= -\frac{\mu}{\hbar^2 k}\int_{r_c}^{\infty} \frac{rU(r)}{\sqrt{r^2 - r_c^2}}dr. \qquad (9)$$

Furthermore, we have adopted a cylindrical coordinate system and decomposed the vector r as $r = r_c + z\hat{n}$ where the z component of r lies along $\hat{n}$ and r_c is perpendicular to $\hat{n}$. We may, therefore, write Eq.(9) as

$$\delta(r_c) = -\frac{\mu}{\hbar^2 k}\int_0^{\infty} U(\sqrt{r_c^2 + z^2})dz. \qquad (10)$$

This is a phase shift for Coulomb-modified eikonal approximation. By taking $U(r)$ as the optical Woods-Saxon forms given by

$$U(r) = -\frac{V_0}{1 + e^{(r-R_v)/a_v}} - i\frac{W_0}{1 + e^{(r-R_w)/a_w}}, \qquad (11)$$

TABLE I: Parameters of the fitted Woods-Saxon potential by using the analysis of Coulomb-modified eikonal approximation for the ^{16}O + ^{16}O elastic scattering at E_{lab}= 480 MeV. R_s is the strong absorption radius and σ_{R_s} is reaction cross section calculated from πR_s^2. 10 % error bars are adopted to obtain χ^2/N value.

V_0 (MeV)	r_v (fm)	a_v (fm)	W_0 (MeV)	r_w (fm)	a_w (fm)	R_s (fm)	σ_{R_s} (mb)	σ_R (mb)	χ^2/N
177	0.805	0.816	37.8	1.060	0.741	7.04	1558	1641	6.77

with $R_{v,w} = r_{v,w}(A_1^{1/3}+A_2^{1/3})$, we can use the phase shift Eq.(10) in the general expression for the elastic scattering amplitude, Eqs.(1) and (2).

III. RESULTS AND DISCUSSIONS

As in the preceding section, we have calculated the elastic differential cross sections for ^{16}O + ^{16}O system at $E_{lab} = 480$ MeV by using the Coulomb-modified eikonal phase shift. Table I shows the parameters of the fitted Woods-Saxon potential, which were determined by least square fits. The calculated results of the differential cross sections for the elastic scattering of ^{16}O + ^{16}O system at E_{lab}= 480 MeV are depicted in figure 1 together with those measured experimentally. The experimental data are taken from the work of Khoa *et al.* [10]. Our calculations lead to reasonable predictions for the characteristic refractive pattern observed over the whole angular range in the ^{16}O + ^{16}O system at E_{lab}= 480 MeV.

The transmission function $T_L = 1 - |S_L|^2$ and partial reaction cross sections for ^{16}O + ^{16}O system at E_{lab}= 480 MeV are shown in figure 2. As shown in figure 2(a), the lower partial waves are totally absorbed and the T_L's decrease very rapidly in a narrow localized angular momenta zone. We can see in figure 2(b) that the values of the partial reaction cross section increase linearly up to $L = 54$. Beyond these L-value, the partial reaction cross section decrease quadratically. A further investigation of the situation can be gained by looking at the strong absorption radius (R_s) and the reaction cross section (σ_{R_s}) given in table I. The strong absorption radius is defined as the distance for which $T_L = 1/2$,
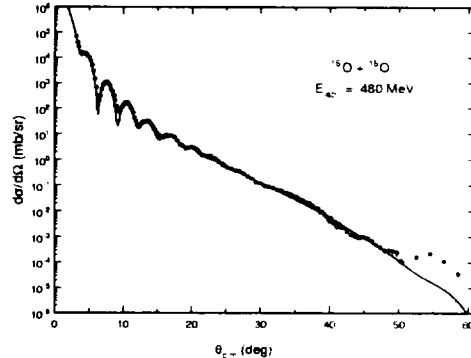

FIG. 1: Elastic scattering angular distributions for ^{16}O + ^{16}O system at E_{lab}= 480 MeV. The solid circles denote the observed data taken from Ref.[10]. The solid curves are the calculated results for Coulomb-modified eikonal approximation.

i.e., the distance where the incident particle has the same probability to be absorbed as to be reflected. The strong absorption radius provides a good estimate of the reaction cross section, $\sigma_{R_s} = \pi R_s^2$.

In order to understand the nature of angular distributions for ^{16}O + ^{16}O system at E_{lab}= 480 MeV, the near- and far-side decompositions of the scattering amplitudes with the Coulomb-modified eikonal approximation were also performed by following the Fuller's formalism [11]. The contribution of the near- and far-side components to the elastic scattering cross sections is shown in figure 3 along with the differential cross sections. The differential cross section is not just a sum of the near- and far-side cross sections but contains the interference between the near- and far-side amplitudes as shown
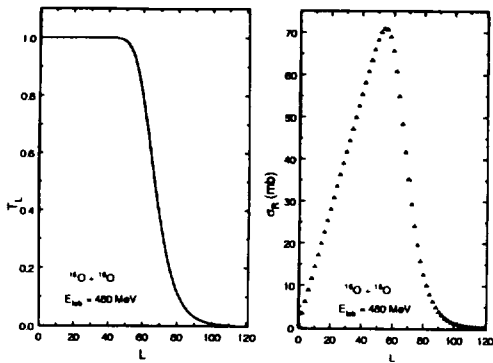
FIG. 2: (a) Transmission function T_L and (b) partial wave reaction cross section σ_L for ^{16}O + ^{16}O system at $E_{lab}=$ 480 MeV plotted versus the orbital angular momentum L.
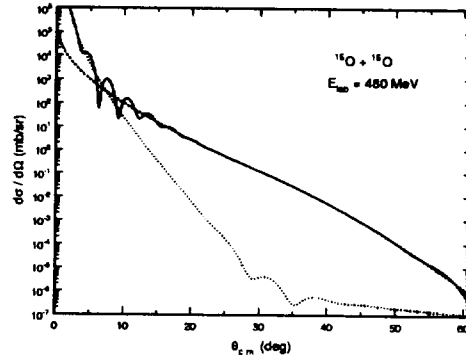
FIG. 3: Differential cross sections (solid curves), near-side contributions (dotted curves), and far-side contributions (dashed curves) obtained by following Fuller's formalism [11] using the Coulomb-modified eikonal approximation for ^{16}O + ^{16}O system at $E_{lab}=$ 480 MeV.

in this figure. The refractive oscillations observed on the elastic scattering angular distribution of ^{16}O + ^{16}O system at $E_{lab}=$ 480 MeV are due to the interferences between the near- and far-side components. The magnitudes of the near- and far-side contributions are equal, crossing point, at $\theta = 7.3°$ for this reaction. However, the far-side contributions to the cross sections dominate at the regions greater than this angle.

It is known that when the absorptive potential is weak and the real potential is strong, the contributions to the scattering from the interior region are large enough to be observed. This features of potential are enough to support nuclear rainbow. The nuclear rainbow angle is obtained from the classical deflection given by

$$\theta_L = 2\frac{d}{dL}(\sigma_L + \mathrm{Re}\ \delta_L).\qquad(12)$$

This deflection angle is a semiclassical treatment of a trajectory with angular momentum L. In a rainbow situation, the strong nuclear force attracts the projectiles towards the scattering center and deflects them to negative scattering angles, which correspond to the region of the rainbow maximum.

As shown in table I, the absorption in ^{16}O + ^{16}O system at $E_{lab}=$ 480 MeV is weak

enough to allow refracted projectiles to populate the elastic channel and typical nuclear rainbow effects could be observed in the angular distribution. In figure 4, we can find the nuclear rainbow angle value $\theta_{nr} = -39.1°$ for the ^{16}O + ^{16}O system at $E_{lab}=$ 480 MeV, which evidently prove a presence of the nuclear rainbow with unambiguous clarity in this system.

In order to know the features of optical potential, we plot in figure 5, the real and imaginary parts of optical potentials, and the "reduced imaginary potential", $w(r)$, i.e., the ratio of the imaginary to real parts of the optical potential. In this figure 5(a), the solid and dashed curves are the real and imaginary parts of optical potentials $U(r)$, respectively. As shown in this figure, the real potential is very strong compared to imaginary one. The imaginary potential itself provides the radial weighting of flux removal or absorption from the entrance channel. The $w(r)$ curves show remarkable for three characteristics. For small r values, imaginary potential is very weak compared to real potential, particularly, $w(0) = 0.21$. This implies deep, elastic interpenetration of the target and projectile, and a feature unambiguously required by the
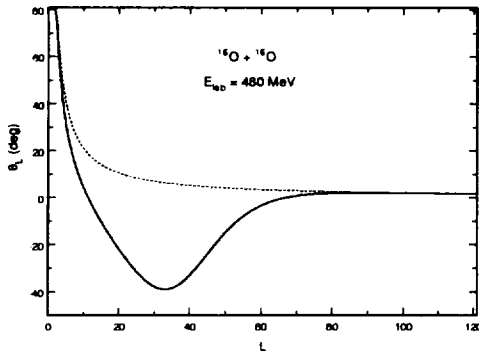
FIG. 4: Deflection functions for ^{16}O + ^{16}O system at E_{lab}= 480 MeV plotted versus the orbital angular momentum L. The dashed curve represents the deflection for the Coulomb phase shift.
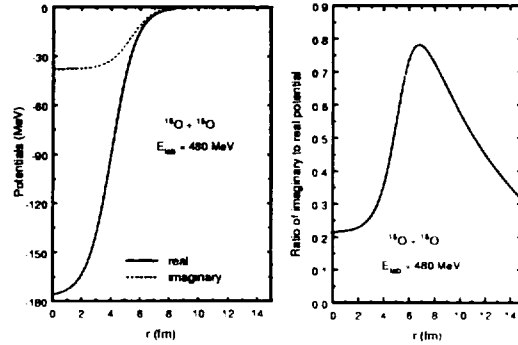

FIG. 5: (a) Real (solid curve) and imaginary (dashed curve) parts of optical potential for the ^{16}O + ^{16}O system at E_{lab}= 480 MeV; (b) Ratio of imaginary to real parts of optical potential.

appearance of nuclear rainbows in the angular distributions. The refractive pattern at large angles is sensitive to the real heavy-ion potential at small radii. As a result the projectile ion can penetrate the nuclear surface barrier of the target, and the cross section becomes sensitive to the value of the real potential in the central region. In the large r range, both real and imaginary parts of potential have exponential tails, with quite different decay lengths with $a_v > a_w$. On the other hand, in the near surface, the pronounced maximum in $w(r)$, with a peak value 0.78, occurs for ^{16}O + ^{16}O system at E_{lab}= 480 MeV. The location of maximum exist close to the "strong absorption radius", R_s, somewhat larger than R_w. The essential conditions which produce the $w(r)$ maximum for this potentials are $R_w > R_v$ and $a_w < a_v$. The appearance of a maximum is not affected by the value of W_0/V_0, though the height of the maximum is, of course, proportional to it. Under these conditions, the maximum occurs at an r value somewhat larger than R_w.

IV. CONCLUDING REMARKS

In this paper, we have analyzed the elastic scattering of ^{16}O + ^{16}O system at E_{lab}=

480 MeV by using the eikonal approximation based on the Coulomb trajectories of colliding nuclei. The present calculations reproduce satisfactorily the characteristic refractive patterns observed in this system. The partial reaction cross section increase linearly up to $L = 54$. Beyond this L value, the partial reaction cross sections have decrease quadratically. We have obtained the nuclear rainbow angle values $\theta_{nr} = -39.1°$ for the ^{16}O + ^{16}O system at E_{lab}= 480 MeV, which evidently prove a presence of the nuclear rainbow in this system. Through near- and far-side decompositions of the cross section, we have shown that the refractive oscillations of ^{16}O + ^{16}O system are due to the interference between the near- and far-side amplitudes. We have obtained the optical potential with strongly real and weakly imaginary parts. This major features support the presence of nuclear rainbows in angular distribution of this system. The ratio of imaginary to real parts of the potential are found to be small in the central regions, indicating weak imaginary potential compared to real potential. This implies deep, elastic interpenetration of the target and projectile. We can see that the refractive part, dominated by the far-side component of the scattering amplitude is sensitive to

the real heavy-ion optical potential at small radii. In the large r range, both real and imaginary parts of potential have exponential tails, with quite different decay lengths with $a_v > a_w$. In the surface region, the pronounced maximum in $w(r)$ occur, the location of maximum exist close to the strong absorption radius of the scattering system. The essential conditions producing the maximum are not W_0/V_0 but $R_w > R_v$ and $a_w < a_v$.

REFERENCES

[1] , E. Stiliaris, H. G. Bohlen, P. Fröbrich, B. Gebauer, D. Kolbert, W. von Oertzen, M. Wilpert and Th. Wilpert, Phys. Lett. 223, 291 (1989).

[2] A. Ingemarsson and G. Fäldt, Phys. Rev. C48, R507 (1993); A. Ingemarsson, Phys. Rev. C56, 950 (1997).

[3] M. E. Brandan and K. W. McVoy, Phys. Rev. C55, 1362 (1997).

[4] S. M. Eliseev and K. M. Hanna, Phys. Rev. C56, 554 (1997).

[5] T. W. Donnelly, J. Dubach and J. D. Walecka, Nucl. Phys. Nucl. Phys. A232, 355 (1974).

[6] G. Fäldt, A. Ingemarsson and J. Mahalanabis, Phys. Rev. C 46, 1974 (1992).

[7] M. H. Cha and Y. J. Kim, Phys. Rev. C51, 212 (1995).

[8] C. E. Aguiar, F. Zardi and A. Vitturi, Phys. Rev. C56, 1511 (1997).

[9] Y. J. Kim, M. H. Cha, Int. J. Mod. Phys. E9, 67 (2000).

[10] D. T. Khoa, W.von Oertzen, H. G. Bohlen, G. Bartnitzky, H. Clement, Y. Sugiyama, B. Gebauer, A. N. Ostrowski, Th. Wilpert and C. Langner, Phys. Rev. Lett. 74, 34 (1995).

[11] R. C. Fuller, Phys. Rev. C12, 1561 (1975).

[12] C. K. Chan, P. Suebka and P. Lu P, Phys. Rev. C 24, 2035 (1981).

[13] D. M. Brink, *Semi-Classical Methods for Nucleus-Nucleus Scattering* (Cambridge Univ. Press, Cambridge, 1985), p.37.